ISBN: 978-3-95450-223-3 ISSN: 2673-7000 doi:10.18429/JACoW-NAPAC2019-WEPLS02

SIMULATION OF A KLYSTRON INPUT CAVITY USING A STEADY-STATE FULL-WAVE SOLVER

A.R. Gold*, S.G. Tantawi
SLAC National Accelerator Laboratory, Menlo Park, USA

Abstract

The simulation of vacuum electronic radio-frequency (RF) power sources is generally done through semi-analytical modeling approaches. These techniques are computationally efficient as they make assumptions on the source topology, such as the requirement that the electron beam travel longitudinally and interact with cylindrical modes. To simulate more general interactions, transient particle-in-cell (PIC) codes are currently required. We present here simulation results of a 5045 klystron using a newly developed steady state code which does not make assumptions on the beam configuration or geometry of the structure and resonant modes. As we solve directly for the steady-state system dynamics, this approach is computationally efficient yet, as demonstrated through comparison with experimental results, provides similar accuracy.

INTRODUCTION

Modeling the non-linear interaction between intense charged particle beams and electromagnetic fields in beam-based radiation sources, from klystrons to free electron lasers, has historically been addressed using semi-analytical simulation tools. Through recent advances in manufacturing and materials science, we can now realize structures and interaction topologies which are vastly more complex than in current devices – unintuitive configurations with the potential to overcome traditional limits in interaction efficiency and output power. These device concepts lie beyond the assumptions of semi-analytical models and existing large signal codes [1–9], however. Their multi-scale nature, spanning time scales from picoseconds to milliseconds, also renders them computationally intractable to model with more general, transient solvers (particle-in-cell codes) [10–13].

To address this issue, we have developed a steady-state solver which accounts for fully general beam-wave interactions. This approach is also computationally efficient, converging to the steady-state solution in less than ten iterations compared to the thousands to billions of time steps required by a transient solver. We describe this steady-state framework and demonstrate how it works through the example of the SLAC 5045 klystron.

STEADY-STATE FRAMEWORK

The basic concept is to iterate on the steady-state solution for the electromagnetic fields and beam evolution through the vacuum structure, eventually obtaining a self consistent solution. The process begins by meshing the structure geometry spatially, after which the resonant frequencies of the structure are identified through an eigenmode analysis. Once these are known, the amplitude of the fields excited by external pre-defined drivers (RF ports, magnets and applied potentials) are computed.

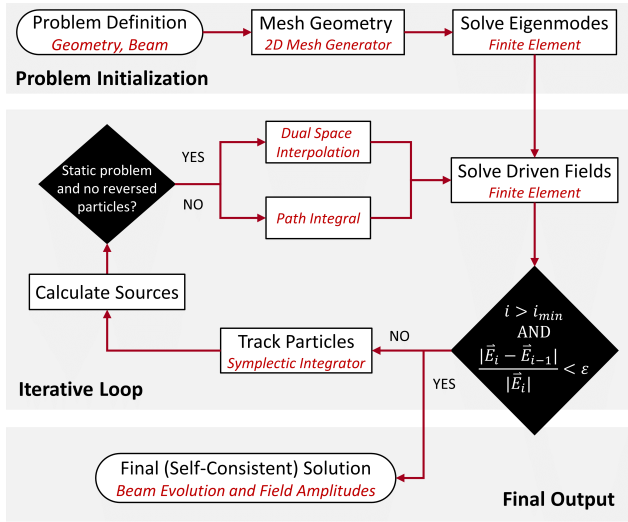

Figure 1: An iterative steady-state beam-wave solver.

In the first iteration, the self-fields of the beam are neglected. Macro-particles, each representing many individual electrons, are tracked through the excited fields to determine the beam evolution. These particles need to be tracked starting from various injection times as the trajectories are dependent on the RF phase at injection. Piece-wise continuous distributions for the charge and current density, ρ and $\vec{J}$ are then calculated from these discrete trajectories. As the fields are computed in the frequency domain, it is in fact the the Fourier transforms, $\tilde{\rho}$ and $\vec{\tilde{J}}$ that are required (in particular, the harmonic content at DC and the resonant frequencies of the structure). Two methods for computing the source terms are used in the solver at present, a dual space interpolation technique for static problems and a path integral (charge deposition) approach for time harmonic problems [14]. The computed distributions become additional driving terms in the next iteration of the field solver.

The process described above is iterated until a self-consistent solution is obtained where the fields produce a beam which generates the same fields. Figure 1 illustrates this process where $i_{min} \geq 1$ is some minimum number of

* vrielink@stanford.edu

ISBN: 978-3-95450-223-3 ISSN: 2673-7000 doi:10.18429/JACoW-NAPAC2019-WEPLS02

iterations and the error in the fields is used to determine convergence.

In addition to applying this steady-state framework to time harmonic problems for the first time, there are other novel aspects to our approach which are amenable to RF source design. The underlying mathematical formulation capturing the beam-wave interaction is not derived from Maxwell's equations directly, as in conventional field solvers. Rather, we employ the classical field theory Lagrangian with an additional gauge fixing term [15, 16]. This Lagrangian approach is particularly well suited to the modeling of beam-wave interactions as it directly accounts for both ρ and $\vec{J}$. This ensures that the self-generated fields due to the electron beam are accurately modeled, a challenge when discrete charge conservation is not guaranteed [17–21].

The advantage to the steady-state approach over existing large signal solvers is that it provides a full-wave solution for the fields and makes no assumptions on the beam evolution or the field profile. In this respect it is similar to a PIC code, but by solving directly for the steady-state response, the number of times the fields and source distribution need to be computed is orders of magnitude fewer. Another advantage is the use of the finite element method (FEM) instead of the finite difference method in solving for the fields. For curved, multi-scale geometries, often encountered in RF sources, FEM provides better solution accuracy for a given problem size.

The improved computational performance does come at a cost: the transient behavior of the device is not solved for. In the limit where the discrete frequencies included in the simulation approach the continuous spectrum of the problem, the full dynamics are captured. However, it is only computationally efficient if relatively few frequencies are included. As the beam-wave interaction in RF sources is resonant at specific frequencies it is usually acceptable to only solve at these frequencies. There are effects, such as non-stationary and parasitic oscillations, that would require including additional frequencies though. Another possible issue is that the steady-state approach assumes that only one steady-state solution exists for a given set of initial parameters. This is not always true, for example in chaotic systems and when the device is sensitive to transient perturbations during start-up. This behaviour should manifest in a sensitivity analysis.

5045 SIMULATION

The SLAC 5045 klystron [22, 23] is a long-standing tube, in operation for over 25 years and is thus a good choice for benchmarking the code. It operates at 2.856 GHz, producing 65 MW of output power from a 350 kV, 415 A beam. We use the steady-state solver to simulate beam-loading in the input cavity of the klystron and compare with experimental results. Given the variation in quality factor and resonant frequency of the manufactured 5045 input cavities and the fact the measurements had to be made on an operating tube where additional components such as coaxial cables and RF windows affected the measurement, perfect agreement is not expected however we obtain reasonable agreement.

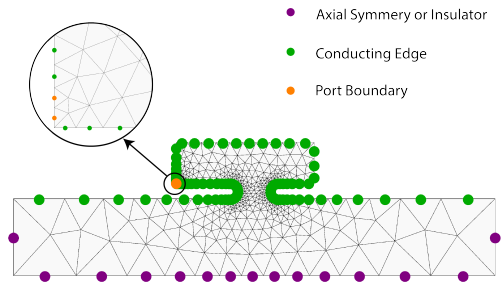

Figure 2: Cross-sectional view of the 5045 input cavity with the mesh and boundary conditions shown. The equivalent (revolved) RF port needs to be very small to produce the same coupling as a 3D rectangular port.

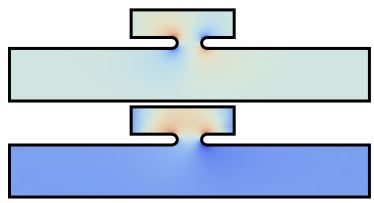

Figure 3: First and second modes of the 5045 input cavity.

The cross-sectional problem geometry is shown in Fig. 2. The problem is azimuthally symmetric and the first two resonant modes of the structure are shown in Fig. 3. The fundamental mode is at 2.86 GHz and the next mode is at 5.13 GHz, far enough away such that it will not be excited by the RF drive power although it could be excited by the beam. The fundamental mode is driven through an azimuthally symmetric RF port, magnified in Fig. 2, designed to ensure a loaded quality factor of 175, the design specification.

The input electron beam is a DC beam which generates strong self-fields. The driving terms in the FEM solver resulting from the beam are plotted in Fig. 4. As expected, the DC contribution is relatively constant over the domain while the RF driving term increases after the cavity due to the induced energy modulation in the beam. The resulting RF fields add to the port-driven fields to produce better matching at the port.

To account for the beam fields, we iterate on the solution. The S11 parameter, or reflection coefficient, of the input

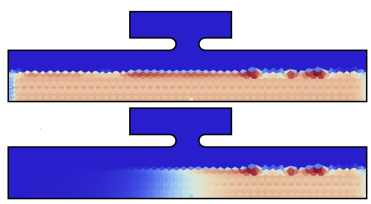

Figure 4: Absolute value of certain components of the finite element drive vector: that which drives ϕ at DC (top) and A_z at the fundamental harmonic (bottom).

ISBN: 978-3-95450-223-3 ISSN: 2673-7000 doi:10.18429/JACoW-NAPAC2019-WEPLS02

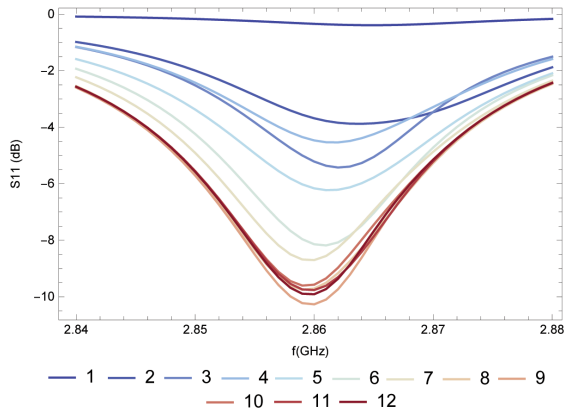

Figure 5: S11 of the 5045 input cavity with beam loading. Each curve corresponds to an iteration of the steady-state solver as shown by the legend on the right.

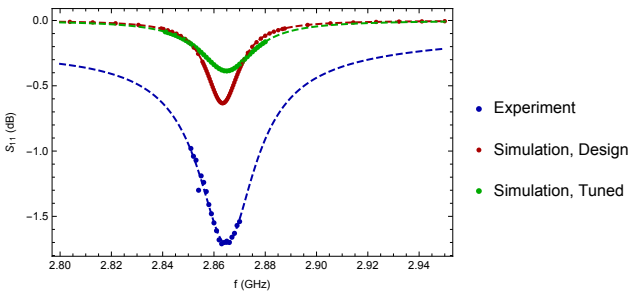

Figure 6: Cold (without beam) S11 as a function of frequency, for the actual device (experiment), the simulated device using design parameters (simulation, design) and the simulated device using the extracted characteristics of the actual device (simulation, tuned).

port is plotted as a function of frequency for each iteration in Fig. 5, demonstrating convergence of the solution already by iteration number 10.

This final solution can be compared with experimental data from an actual 5045. The cold test S11, Fig. 6, is influenced by some of the other RF components (for example the losses in the coaxial cable). We can account for this by applying a Lorentzian fit that includes background and skew effects, as is done in Ref. [24]. Removing these effects results in Fig. 7. The quality factor obtained is Q = 113, close to the value of 110 measured during the original cold test. We re-tuned the cavity in simulation to more closely match the characteristics of the real cavity and use this in comparing the hot test measurements (those with beam included).

Assuming the skew and background parameters are the same in the hot test measurement, a reasonable assumption if they are not a function of the input or reflected power, we can apply the same correction to our hot test results, shown without correction in Fig. 8. This produces Fig. 9, which both matches the approximate value of around -12 dB (decibels) recorded for most tubes at the drive frequency, and agrees reasonably well with the steady-state solver output.

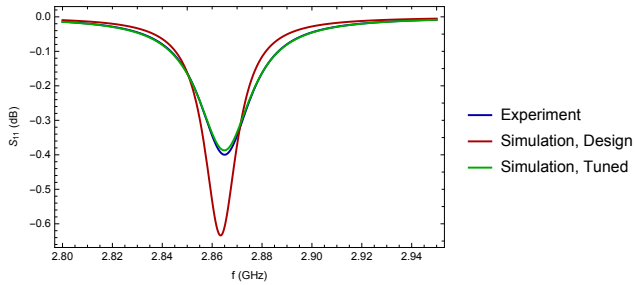

Figure 7: Cold (without beam) S11 as a function of frequency similar to Fig. 6 but where the skew and background have been removed from the experimental data.

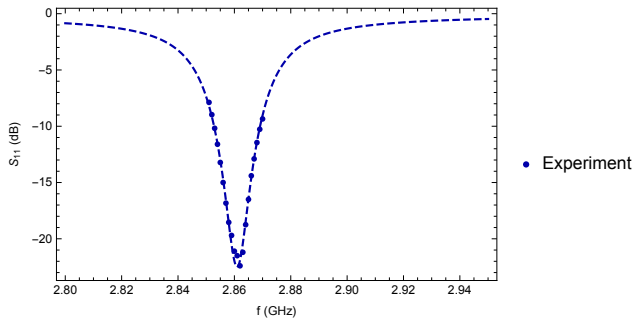

Figure 8: Hot (with beam) S11 as a function of frequency without any correction to the experimental data.

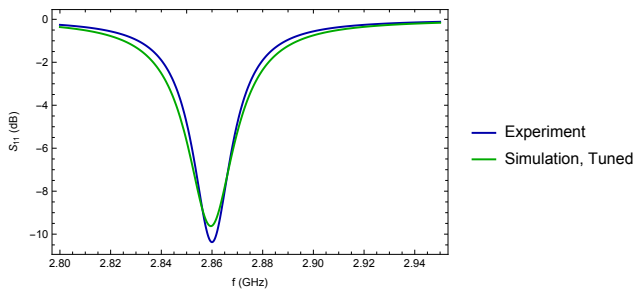

Figure 9: Hot (with beam) S11 as a function of frequency applying the same correction to the experimental data as in Fig. 7 and comparing with simulation.

CONCLUSION

We have developed and demonstrated a steady-state time harmonic beam-wave interaction solver for RF sources. Our approach is both computationally efficient, solving for the fields in the frequency domain using FEM, and capable of accounting for general beam-wave interactions.

A preliminary benchmarking example is provided here for the 5045 klystron. Future work will look to make more robust comparisons with experimental data for devices where the operating conditions can be better controlled, as well as comparisons with existing large signal codes and for more exotic RF source topologies, with PIC codes.

ACKNOWLEDGMENT

This project was funded by U.S. Department of Energy under Contract No. DE-AC02-76SF00515.

ISBN: 978-3-95450-223-3 ISSN: 2673-7000 doi:10.18429/JACoW-NAPAC2019-WEPLS02

REFERENCES

[1] J. Cai and I. Syratchev, "KlyC. The 1D/1.5D large signal computer code for the klystron simulations. User manual.," CERN, Geneva, Tech. Rep. CERN-ACC-2018-0050. CLIC-Note-1137, Oct. 2018.

[2] J. Cai and I. Syratchev, "Klyc: 1.5-d large-signal simulation code for klystrons," *IEEE Transactions on Plasma Science*, vol. 47, no. 4, pp. 1734–1741, Apr. 2019. DOI: 10.1109/TPS.2019.2904125.

[3] A. N. Vlasov, T. M. Antonsen, D. P. Chemin, B. Levush, K. T. Nguyen, and S. J. Cooke, "Tesla: Large signal simulation code for klystrons," in *Fifth IEEE International Vacuum Electronics Conference (IEEE Cat. No.04EX786)*, Apr. 2004, pp. 314–315. DOI: 10.1109/IVELEC.2004.1316337.

[4] P. Tien, "A large signal theory of traveling wave amplifiers," *Bell System Technical Journal*, vol. 35, no. 2, pp. 349–374, 1956. DOI: 10.1002/j.1538-7305.1956.tb02386.x.

[5] A. N. Vlasov, T. M. Antonsen, I. A. Chernyavskiy, D. P. Chernin, and B. Levush, "A computationally efficient two-dimensional model of the beam–wave interaction in a coupled-cavity twt," *IEEE Transactions on Plasma Science*, vol. 40, no. 6, pp. 1575–1589, Jun. 2012. DOI: 10.1109/TPS.2012.2188547.

[6] M. Botton, T. M. Antonsen, B. Levush, K. T. Nguyen, and A. N. Vlasov, "Magy: A time-dependent code for simulation of slow and fast microwave sources," *IEEE Transactions on Plasma Science*, vol. 26, no. 3, pp. 882–892, Jun. 1998. DOI: 10.1109/27.700860.

[7] S. Sabchevski, T. Idehara, T. Saito, I. Ogawa, S. Mitsudo, and Y. Tatematsu, "Physical models and computer codes of the gyrosim (gyrotron simulation) software package," *FIR Center Report FIR FU*, vol. 99, 2010.

[8] K. Avramides, I. Pagonakis, C. Iatrou, and J. Vomvoridis, "Euridice: A code-package for gyrotron interaction simulations and cavity design," *EPJ Web of Conferences*, vol. 32, no. 2012, pp. 04016/1–6, 2012, 31.30.03; LK 01. DOI: 10.1051/epjconf/20123204016.

[9] S. Alberti, T. M. Tran, K. A. Avramides, F. Li, and J. .-.-. Hogge, "Gyrotron parasitic-effects studies using the time-dependent self-consistent monomode code twang," in *2011 International Conference on Infrared, Millimeter, and Terahertz Waves*, Oct. 2011, pp. 1–2. DOI: 10.1109/irmmw-THz.2011.6105097.

[10] B. Goplen, L. Ludeking, D. Smith, and G. Warren, "User-configurable magic for electromagnetic pic calculations," *Computer Physics Communications*, vol. 87, no. 1, pp. 54–86, 1995, Particle Simulation Methods. DOI: 10.1016/0010-4655(95)00010-D.

[11] *Cst studio suite 20178 user's manual*, English, CST Studio Suite, 2018. https://www.cst.com 2018.

[12] A. Candel *et al.*, "Parallel finite element particle-in-cell code for simulations of space-charge dominated beam-cavity interactions," in *2007 IEEE Particle Accelerator Conference (PAC)*, Jun. 2007, pp. 908–910. DOI: 10.1109/PAC.2007.4440757.

[13] D. Grote, A. Friedman, J. Vay, and I. Haber, "The warp code: Modeling high intensity ion beams," *AIP Conference Proceedings*, vol. 749, no. 1, pp. 55–58, 2005. DOI: 10.1063/1.1893366.

[14] A. Gold and S. Tantawi, "Efficient dual space source interpolation method for the numerical solution of self-consistent static beam-wave interactions," *Phys. Rev. Accel. Beams*, vol. 21, p. 114 403, 11 Nov. 2018. DOI: 10.1103/PhysRevAccelBeams.21.114403.

[15] A. Gold and S. Tantawi, "A classical field theory formulation for the numerical solution of time harmonic electromagnetic fields," *arXiv preprint arXiv:1902.01805*, 2019.

[16] A. Vrielink, M. Nasr, and S. Tantawi, "Derivation of a Finite Element Formulation From a Lagrangian for the Electromagnetic Potentials," in *Proceedings, 8th International Particle Accelerator Conference (IPAC 2017): Copenhagen, Denmark, May 14-19, 2017*, 2017, WEPIK111. DOI: 10.18429/JACoW-IPAC2017-WEPIK111.

[17] B. Marder, "A method for incorporating gauss' law into electromagnetic pic codes," *Journal of Computational Physics*, vol. 68, no. 1, pp. 48–55, 1987. DOI: 10.1016/0021-9991(87)90043-X.

[18] B. Langdon, "On enforcing gauss' law in electromagnetic particle-in-cell codes," *Computer Physics Communications*, vol. 70, no. 3, pp. 447–450, 1992. DOI: 10.1016/0010-4655(92)90105-8.

[19] P. Ciarlet and S. Labrunie, "Numerical analysis of the generalized maxwell equations (with an elliptic correction) for charged particle simulations," *Mathematical Models and Methods in Applied Sciences*, vol. 19, no. 11, pp. 1959–1994, 2009. DOI: 10.1142/S0218202509004017.

[20] R. Barthelme', P. Ciarlet, and E. Sonnendru:cker, "Generalized formulations of maxwell's equations for numerical vlasov-maxwell simulations," *Mathematical Models and Methods in Applied Sciences*, vol. 17, no. 05, pp. 657–680, 2007. DOI: 10.1142/S0218202507002066.

[21] P. Ciarlet, H. Wu, and J. Zou, "Edge element methods for maxwell's equations with strong convergence for gauss' laws," *SIAM Journal on Numerical Analysis*, vol. 52, no. 2, pp. 779–807, 2014. DOI: 10.1137/120899856.

[22] A. Beebe *et al.*, "25 year performance review of the slac 5045 s-band klystron," in *Conf. Proc.*, vol. 110904, 2011, pp. 409–411.

[23] M. Allen, W. Fowkes, R. Koontz, H. Schwarz, J. Seeman, and A. Vlieks, "Performance of the slac linear collider klystrons," in *Conf. Proc.*, vol. 870316, 1987, p. 1713.

[24] P. Petersan and S. Anlage, "Measurement of resonant frequency and quality factor of microwave resonators: Comparison of methods," *Journal of applied physics*, vol. 84, no. 6, pp. 3392–3402, 1998.